A TECHNICAL MEMORANDUM

NASA TM X-2323

CASE FILE COPY

# LIMINARY INVESTIGATION GASEOUS EMISSIONS FROM ENGINE AFTERBURNERS

arry A. Diehl

Research Center

land, Ohio 44135

AL AERONAUTICS AND SPACE ADMINISTRATION • WASHINGTON, D. C. • JULY 1971

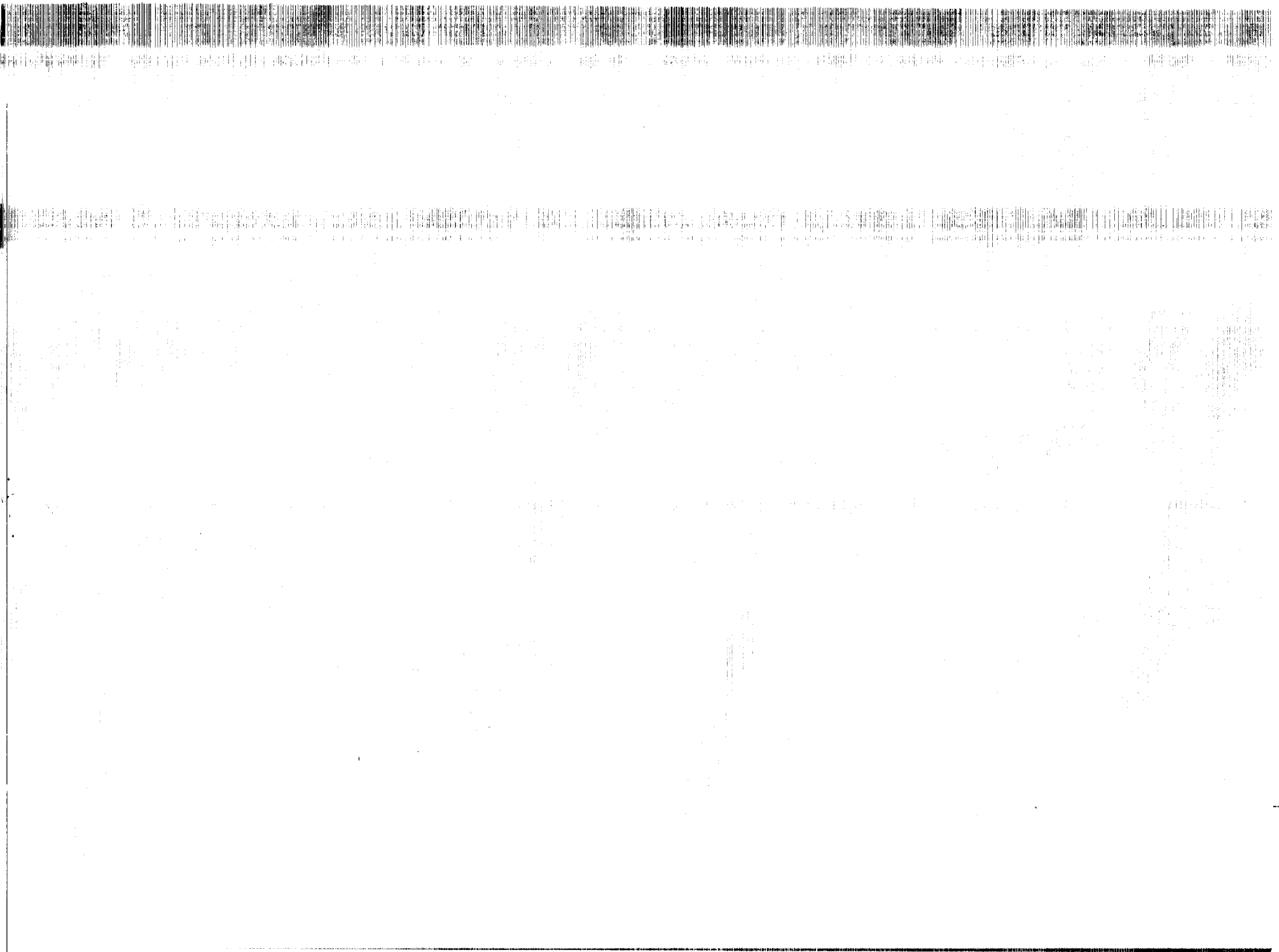

| 1. Report No. | 2. Government Accession No. | 3. Recipient's Catalog No. |
|---|---|---|
| NASA TM X-2323 | | |

| 4. Title and Subtitle | 5. Report Date |
|---|---|
| PRELIMINARY INVESTIGATION OF GASEOUS EMISSIONS FROM JET ENGINE AFTERBURNERS | July 1971 |
| | 6. Performing Organization Code |
| 7. Author(s) | 8. Performing Organization Report No. |
| Larry A. Diehl | E-6256 |
| | 10. Work Unit No. |
| 9. Performing Organization Name and Address | 720-03 |
| Lewis Research Center<br>National Aeronautics and Space Administration<br>Cleveland, Ohio 44135 | 11. Contract or Grant No. |
| | 13. Type of Report and Period Covered |
| 12. Sponsoring Agency Name and Address | Technical Memorandum |
| National Aeronautics and Space Administration<br>Washington, D.C. 20546 | 14. Sponsoring Agency Code |

15. Supplementary Notes

16. Abstract

Gaseous emissions from jet engine afterburners were measured over a range of fuel-air ratios. The two configurations used were a full-size turbofan engine with an afterburner and a 51-cm (20-in.) diameter research afterburner. Nitric oxide emission did not increase with afterburning. The maximum nitric oxide concentration measured with afterburning was 3.4 g/kg of fuel burned while the maximum measured carbon monoxide emission was 1300 g/kg of fuel burned. Appreciable quantities of unburned hydrocarbons resulted from operation at high fuel-air ratios. Nitric oxide concentrations were less than theoretical equilibrium values by as much as two orders of magnitude; concentrations of unburned products were always greater than equilibrium values.

| 17. Key Words (Suggested by Author(s)) | 18. Distribution Statement |
|---|---|
| Air pollution; Afterburning; Combustion; Combustion products; Exhaust gases; Exhaust products; Fuel combustion; Jet engines; Gas turbine engines; Thrust augmentation | Unclassified - unlimited |

| 19. Security Classif. (of this report) | 20. Security Classif. (of this page) | 21. No. of Pages | 22. Price* |
|---|---|---|---|
| Unclassified | Unclassified | 18 | $3.00 |

*For sale by the National Technical Information Service, Springfield, Virginia 22151

# PRELIMINARY INVESTIGATION OF GASEOUS EMISSIONS FROM JET ENGINE AFTERBURNERS

by Larry A. Diehl

Lewis Research Center

## SUMMARY

Gaseous emissions from jet engine afterburners were measured over a range of fuel-air ratios. The two configurations used were a full-size turbofan engine with afterburner and a 51-centimeter (20-in.) diameter research afterburner. The inlet conditions to the engine afterburner were an average total temperature of 660 K (730° F), an average velocity of 132 meters per second (435 ft/sec), and a pressure of 1 atmosphere. Research afterburner inlet conditions were a total temperature of 920 K (1200° F), a velocity of 150 meters per second (500 ft/sec), and a static pressure of 1 atmosphere. Gas samples collected at the afterburner exit were analyzed for nitric oxide, carbon monoxide, unburned hydrocarbons, hydrogen, and carbon dioxide.

In general the data trends with increasing fuel-air ratio were similar for both the full size and research afterburner. Nitric oxide emission did not increase with afterburning. The maximum concentration measured with afterburning was 3.4 grams per kilogram of fuel burned. Afterburners proved to be heavy producers of carbon monoxide with values as high as 1300 grams per kilogram of fuel burned being recorded. Appreciable quantities of unburned hydrocarbons resulted from operation at high fuel-air ratios.

The measured values show that equilibrium calculations alone are not sufficient to predict engine emissions. Measured concentrations of nitric oxide at high fuel-air ratios were less than the equilibrium values by at least two orders of magnitude. Because of inefficient operation, measured values of unburned product concentrations were always greater than the equilibrium value.

## INTRODUCTION

Public concern over pollutants from aircraft jet engines has stimulated a good deal of research in this area. Although information concerning emissions from dry engines is

available (see, e.g., refs. 1 to 4), there are little published data concerning the effect of afterburning on these emissions. With a commercial application, such as the supersonic transports, the amount of fuel consumed by jet engine afterburning would increase considerably.

It is generally acknowledged that a jet engine afterburner is potentially a heavy polluter. This is due both to its general level of inefficiency as well as its large fuel consumption during operation. The purpose of this report is to document the emissions from typical present-day afterburners. No attempt is made to assess the environmental effects of these emissions; rather, such discussions may be found in references 5 and 6.

Measurements of afterburner emissions were made on a TF30-P-3 twin-spool turbofan equipped with an afterburner. Additional data were obtained from a research afterburner consisting of various configurations mounted in a 51-centimeter (20-in.) connected-duct facility. A comparison is drawn between the full-size engine and a circular two-ring V-gutter. Supporting data from the remaining research afterburner configurations are presented in an overall envelope curve. Samples taken were analyzed for nitric oxide, carbon monoxide, unburned hydrocarbons, hydrogen, and carbon dioxide. No measurements were made of particulate emissions. For both configurations an ASTM A-1 fuel was used, and a range of fuel-air ratios was investigated.

# APPARATUS

## Engine and Facility

The engine used in this investigation was a twin-spool turbofan equipped with an afterburner (Pratt & Whitney TF30-P-3). The engine was installed in an altitude test chamber that could be evacuated to the desired pressure. Conditioned air was supplied to the engine through the laboratory's connected duct system. Further details of engine and facility may be found in reference 7. The thrust stand was not used during these runs, and no measurement of efficiency was made.

A schematic of the engine afterburner and sample probe location is shown in figure 1. The afterburner consists of a five-zone staged-fuel injection system. Which zones are operating is programmed by the engine throttle setting. The gas-sampling probe was an existing water-cooled total pressure rake. Twelve sampling points, located at centers of equal area were connected to a common manifold at the rake exit. The 12-point rake samples an area equal to the nozzle area in its closed position.

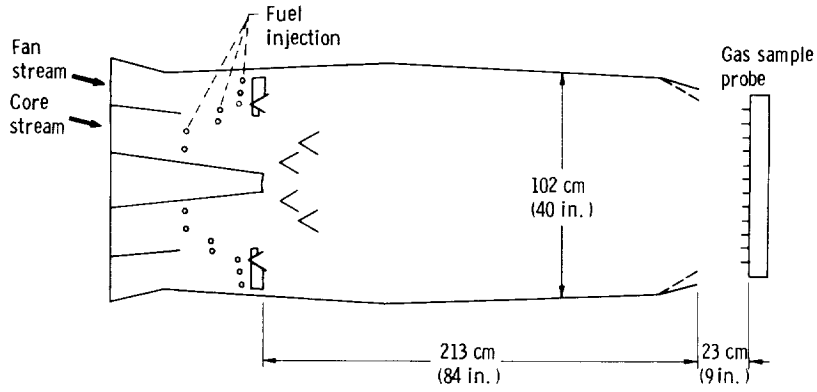


Figure 1. - TF 30-P-3 afterburner.

## Research Afterburner and Facility

The research afterburner consisted of various flameholder configurations mounted in a 51-centimeter (20-in.) connected duct facility. An indirect-fired preheater provided conditioned air at 450 K (350$^{O}$ F). Conditions simulating an afterburner inlet were provided by a direct-fired preheater consisting of four J-57 combustor cans fueled with clear gasoline. The flameholder configurations were selected from another test program involved with studying advanced afterburner concepts and included swirl cans, film vaporizers, carburetors, and conventional V-gutter types. The afterburner length was fixed at 130 centimeters (51 in.) and was terminated by a set of water spraybars that quenched the reaction. Combustion efficiency was determined by an enthalpy balance technique.

Figure 2 is a schematic of the research afterburner and gas sample probe location. The sample probe was a water-cooled eight-point radial total pressure rake. The sampling points were arranged such that the sample would be center-weighted. The eight sample points were connected to a common manifold at the rake exit.

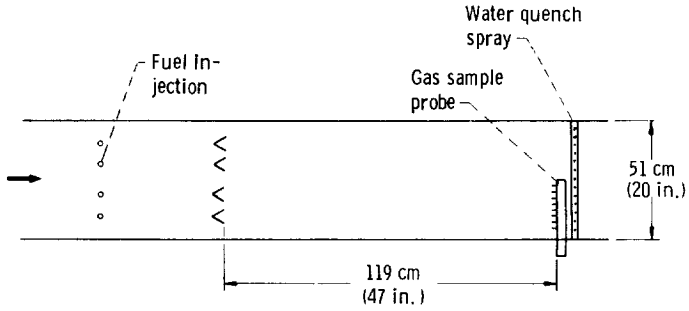


Figure 2. - Research afterburner.

A conventional circular two-ring V-gutter was chosen as a configuration comparable to the TF30-P-3. The gutter rings are 15.2 centimeters (6 in.) and 33 centimeters (13 in.) in diameter, and the gutter width is 3.8 centimeters (1.5 in.). The blocked area is 30.8 percent. Two circular spray rings injected fuel 46 centimeters (18 in.) upstream.

## GAS SAMPLE ACQUISITION AND ANALYSIS

### Gas Sample System

The gas samples were transferred to the analytical instruments by a batch sample technique. The analysis procedures required that two different samples be taken. Nitric oxide samples were gathered in 250 or 500 milliliter glass vessels which had been previously evacuated to 0.050 torr or less. Final sample pressure was 1 atmosphere. For the remaining constituents of interest a diaphragm pump, located downstream from the nitric oxide withdrawal point, was used to pump the gases into 33-liter stainless-steel containers that had been previously evacuated to 1 torr or better. Final sample pressure was nominally 24 newtons per square centimeter (35 psia).

A stainless-steel line was used to transfer the gases from the sample probe to a convenient site for filling the sample bottles. For the research afterburner and for the full size engine these line lengths were approximately 2 meters (7 ft) and 5.5 meters (18 ft), respectively. In order to prevent condensation of water and to minimize the adsorption-desorption effects of hydrocarbon compounds, the line was heated to an average temperature of 450 K (350$^{\circ}$ F). The actual sample gas temperature was monitored near the port where nitric oxide samples were withdrawn. This temperature was kept at 370 K (210$^{\circ}$ F), or slightly higher, whenever possible. Samples were withdrawn only after the pump had been operating for a sufficient time to establish thermal equilibrium and to properly purge the sample line of the previous sample.

### Gas Sample Analysis

Several analysis procedures were used to determine the concentration of the various constituents. Nitric oxide was determined by the Saltzman chemical analysis procedure (ref. 8). Unburned hydrocarbon samples were batch processed through a Beckman model 106E flame ionization detector. The cell was maintained at 367 K (200$^{\circ}$ F), and the gas sample bottle was at ambient temperature. The concentrations of the remaining constituents of interest, CO, $CO_2$, and $H_2$, were determined by a Beckman model GC-4 gas

chromatograph. In all cases the concentrations determined by these analyses are expressed in parts per million by volume (ppm).

Because of the condensation of water vapor in the unheated sample vessels, the measured concentration of the emissions is corrected for the material removed in order to represent the true engine exhaust concentrations. Therefore, the actual concentration of any component [X], in terms of the measured quantity, is given by $[X]_{actual} = [X]_{measured} \times (1 - \text{fraction } H_2O \text{ removed})$. For leaner-than stoichiometric operation the percent water vapor produced is approximately equal to the percent $CO_2$ produced.

## TEST CONDITIONS

### Engine

The afterburner was operated at a variety of fuel-air ratios with a fixed engine setting corresponding to a simulated flight Mach number of 1.3 at an altitude of 12 200 meters (40 000 ft). The primary combustor inlet conditions were a pressure of 8 atmospheres and a temperature of 530 K (500$^{\circ}$ F). The resultant afterburner inlet conditions were a pressure of 1 atmosphere, an average total temperature of 660 K (730$^{\circ}$ F), and an average velocity of 132 meters per second (435 ft/sec). Supplementary emission data were taken at sea-level idle and sea-level takeoff without afterburning. Facility limitations prohibited operation of the afterburner at sea-level conditions.

### Research Afterburner

All research afterburner tests were conducted with the afterburner inlet total temperature at 920 K (1200$^{\circ}$ F). An indirect-fired preheater provided 450 K (350$^{\circ}$ F) air with a vitiating preheater providing the remainder of the required temperature rise. The required preheater fuel-air ratio was 0.012, and the preheater inlet pressure was 13 newtons per square centimeter (19 psia). The afterburner inlet static pressure was fixed at 1 atmosphere by adjusting the duct exhaust butterfly valve. Afterburner inlet velocity was a constant 150 meters per second (500 ft/sec).

## RESULTS AND DISCUSSION

The emission data are presented in two ways. Values of the concentrations in parts per million by volume are contained in tables I and II. These data are shown graphically

TABLE I. - MEASURED GASEOUS EMISSIONS FOR TF30-P-3 ENGINE

| Test condition | Air flow rate | | Fuel flow rate to total air flow rate | | Corrected for $H_2O$ removed | | | | | | | | | |
|---|---|---|---|---|---|---|---|---|---|---|---|---|---|---|
| | | | | | $[NO_x]$ | | [CO] | | [HC] | | $[H_2]$ | | $[CO_2]$ | |
| | kg/sec | lb/sec | Afterburner | Total | ppm | g/kg fuel | ppm | g/kg fuel | ppm C | g/kg fuel | ppm | g/kg fuel | ppm | g/kg fuel |
| Idle | 43.7 | 96.4 | 0 | 0.00249 | 4 | 1.66 | 210 | 81.6 | 103 | 20.0 | 23 | 0.639 | 4 834 | 2952 |
| Takeoff | 105.9 | 233.7 | 0 | .00820 | 62 - 67 | 7.9 - 8.5 | 13 | 1.54 | 42 | 2.49 | 1 | .007 | 20 300 | 3786 |
| Altitude[a] | 53.8 | 118.8 | 0 | .00865 | 65 | 7.84 | 37 | 4.16 | 36 | 2.03 | 1 | .006 | 22 750 | 4024 |
| ↓ | 53.0 | 117.1 | .0080 | .0172 | 55 | 3.36 | 736 | 42.0 | 145 | 4.14 | 22 | .090 | 26 600 | 2386 |
| | 52.3 | 115.4 | .0154 | .0247 | 66 | 2.83 | 852 | 34.1 | 144 | 2.88 | 36 | .103 | 31 900 | 2008 |
| | 52.9 | 116.7 | .0191 | .0282 | 50 | 1.88 | 797 | 28.0 | 122 | 2.15 | 30 | .076 | 32 850 | 1817 |
| | 52.9 | 116.7 | .0294 | .0386 | 48 | 1.34 | 902 | 23.4 | 135 | 1.75 | 38 | .070 | 31 900 | 1302 |
| | 52.3 | 115.2 | .0460 | .0551 | 50 | .99 | 13 530 | 249.5 | 22 | .20 | 2250 | 2.97 | 78 400 | 2277 |

[a]Altitude data were taken at a simulated engine inlet condition of Mach 1.3 flight at 12 200 m (40 000 ft).

TABLE II. - MEASURED GASEOUS EMISSIONS FOR TWO-RING V-GUTTER RESEARCH AFTERBURNER

[Afterburner inlet conditions: Total temperature, 920 K (1200° F); static pressure, 10.0 N/cm$^2$ (14.5 psia); velocity, 150 m/sec (500 ft/sec); air flow rate, 11.3 kg/sec (25 lb/sec).]

| Inner spray ring fuel-air ratio | Outer spray ring fuel-air ratio | Total fuel-air ratio | Total combustion efficiency, percent (a) | Corrected for $H_2O$ removed | | | | | | | | | |
|---|---|---|---|---|---|---|---|---|---|---|---|---|---|
| | | | | $[NO_x]$ | | [CO] | | [HC] | | $[H_2]$ | | $[CO_2]$ | |
| | | | | ppm | g/kg fuel | ppm | g/kg fuel | ppm C | g/kg fuel | ppm | g/kg fuel | ppm | g/kg fuel |
| 0 | 0 | 0.0121 | 97 | 6 | 0.519 | 1 449 | 117.0 | 170 | 6.87 | 107 | 0.618 | ------ | ---- |
| 0 | 0 | .0121 | 97 | 10 | .865 | 1 344 | 108.5 | 247 | 9.98 | 111 | .641 | 22 700 | 2880 |
| 0 | .0216 | .0339 | 91 | 5 | .158 | 3 320 | 97.7 | 1263 | 18.6 | 359 | .755 | ------ | ---- |
| 0 | .0338 | .0458 | 90 | 5 | .118 | 5 390 | 118.8 | 904 | 9.97 | 708 | 1.115 | ------ | ---- |
| 0 | .0459 | .0580 | 92 | 10 | .189 | 13 450 | 237.0 | 868 | 7.65 | 2648 | 3.33 | ------ | ---- |
| .0125 | 0 | .0247 | 88 | 10 | .429 | 2 870 | 114.9 | 504 | 10.1 | 272 | .779 | 51 500 | 3241 |
| 0 | .0162 | .0280 | 88 | 2 | .076 | 3 150 | 111.6 | 911 | 16.2 | 304 | .770 | 42 600 | 2373 |
| 0 | .02817 | .0403 | 92 | 7 | .187 | 4 540 | 113.1 | 1038 | 12.9 | 534 | .951 | 56 500 | 2212 |
| 0 | .02814 | .0402 | 92 | 8 | .214 | 4 530 | 113.1 | 1086 | 13.6 | 546 | .975 | 58 700 | 2304 |
| .0158 | 0 | .0278 | 90 | 9 | .344 | 6 510 | 232.3 | 682 | 12.2 | 1060 | 2.70 | 60 700 | 3404 |
| .0121 | 0 | .0240 | 88 | 8 | .353 | 3 095 | 127.4 | 594 | 12.2 | 293 | .862 | 55 800 | 3612 |
| .0080 | 0 | .0197 | 85 | 5 | .268 | 2 215 | 110.6 | 604 | 15.1 | 193 | .689 | 43 200 | 3392 |

[a]Total combustion efficiency is based on total fuel flow rate.

in terms of the emission index, the number of grams of constituent per kilogram of fuel burned. The emission index can be calculated from the fuel-air ratio and the constituent concentration.

The total fuel-air ratio is computed from the total fuel flow (engine plus afterburner or preheater plus afterburner) and the total airflow rate. The TF30 turbofan engine has a bypass ratio of 1.0, so for nonafterburning conditions the total fuel-air ratio is one-half the core fuel-air ratio.

## Nitric Oxide Emission

The measured values of nitric oxide emission are presented in figure 3. The data shown are for constant primary combustor (engine), or preheater (research afterburner)

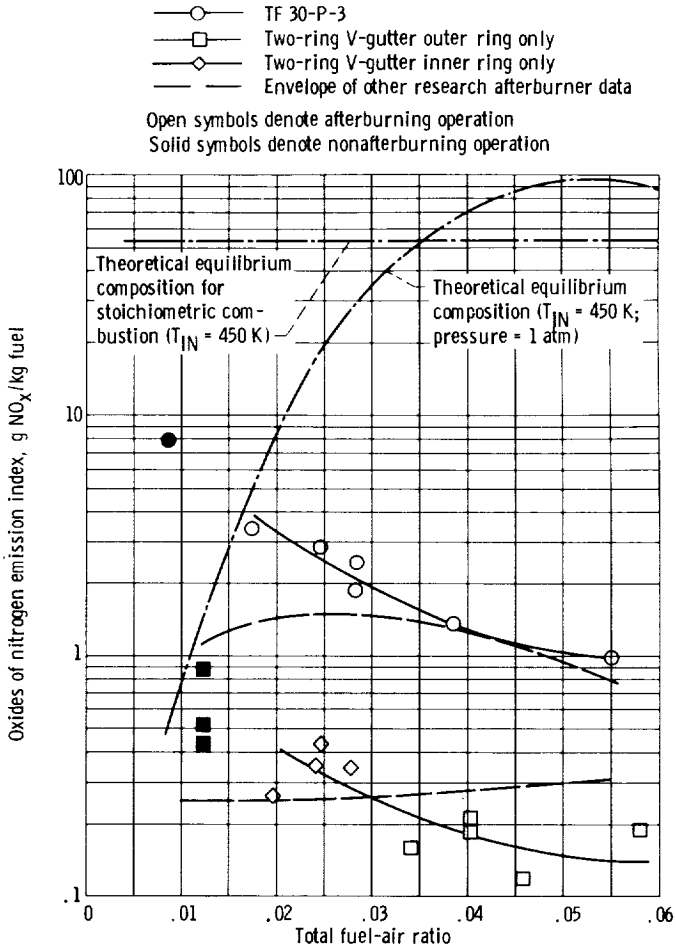


Figure 3. - Oxides of nitrogen emission index.

conditions. The absolute value of the concentration was always less than 70 ppm as shown in tables I and II. Scatter in the research afterburner data is due to errors involved in measuring concentrations of 10 ppm or less.

It is interesting to note that the primary, or preheater, combustion determines the overall NO level. The afterburner has a negligible effect on the concentration. Nearly constant volumetric concentration accounts for the decrease in emission index with increasing fuel-air ratio since emission index is directly proportional to concentration and inversely proportional to fuel-air ratio.

Some justification can be found for the difference in overall level between the J-57 preheater and the TF30 primary combustor. Nitric oxide production is heavily dependent on both temperature and gas residence time in the high-temperature environment. At the operating conditions in question the TF30 primary combustor has approximately twice the gas residence time as well as a higher temperature due to its higher fuel-air ratio. Further, the overall mode of operation of the J-57 preheater, as detailed in the Research Afterburner section, is actually operating in a near idle condition where the NO level is lower (see, e.g., refs. 2 to 4). The fact that the engine afterburner overall gas residence time is also twice the research afterburner value (i.e., 18 versus 8 msec for isothermal inlet conditions) appears to have little effect.

The extent of the deviation from equilibrium conditions is also shown in figure 3. The program used to calculate the equilibrium composition is described in reference 9. For any point on the theoretical curve, the composition is based on equilibrium conditions corresponding to the ideal temperature rise at that particular fuel-air ratio. For low total fuel-air ratios, the measured NO value may exceed the equilibrium value. This is because in the local region where the NO is being formed the combustion is occurring at a near-stoichiometric condition which differs significantly from the overall fuel-air ratio used in the equilibrium calculation. However, for combustion at near-stoichiometric conditions the theoretical equilibrium value is greater than any of the measured values. Jet engine combustors do not allow sufficient residence time for the NO to achieve equilibrium concentrations. Calculations based on reaction kinetics may provide additional insight into the problem. Such an approach has already been tried in references 3 and 10.

## Carbon Monoxide Emission

It was anticipated that measured values of CO emission would exceed the equilibrium predicted concentration because of the inefficient operation of afterburners. Calculations show that for each percent inefficiency due entirely to incomplete combustion of CO, approximately 43 grams of CO per kilogram of fuel burned are produced.

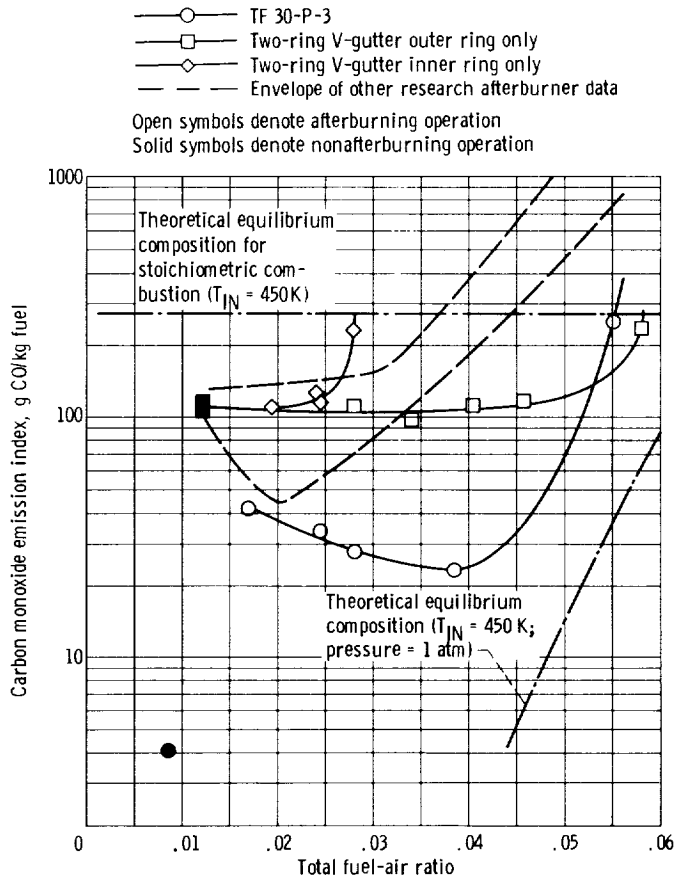


Figure 4. - Carbon monoxide emission index.

The measured values of CO emission shown in figure 4 indicate the wide range in values obtained. For some of the other research afterburner designs (these include swirl cans, film vaporizers, and carburetors) shown in the envelope, the concentration reached nearly 68 000 ppm or, in terms of the emission index, 1300 grams per kilogram of fuel. In general, CO production increased with increasing fuel-air ratio. A case in point is the inner ring operation of the research afterburner two-ring V-gutter. The marked increase in CO production for the inner ring occurs near the rich blowout limit.

The difference in overall emission level between the engine and the research afterburner is, to a large extent, due the difference in the preheater and primary combustor emission levels. Subtracting this reference level from each data set would show the full-scale engine afterburner to be the heavier polluter.

Carbon monoxide emission is always higher than the equilibrium predicted value. For those cases where fuel-air ratio is high, or where efficiency has already peaked, measured values may exceed the equilibrium stoichiometric values.

Kinetics calculations of the CO reaction (ref. 11) show that for temperatures above 1030 K (1400° F) and at atmospheric pressure the reaction is very rapid and thus mixing limited. As the exhaust gas temperature of an afterburner is high, additional reaction may occur in the exhaust plume until sufficient cooling quenches the reaction. Therefore, the actual amount of CO that finally remains may be less than the measured value due to continuing oxidation downstream of the sample probes. The data presented for CO, therefore, are an expected upper limit.

## Unburned Hydrocarbon Emission

The flame ionization detector used to measure unburned hydrocarbons is calibrated to count carbon atoms, and the result is expressed as parts per million carbon (ppm C). It is therefore necessary to make some assumption as to the structure of the unburned hydrocarbon molecule to determine the emission index. The assumed form of unburned hydrocarbons was $CH_2$. Ten grams of unburned hydrocarbon per kilogram of fuel burned would result in a combustion inefficiency of 1 percent. Poor fuel distribution and incomplete mixing are assumed to be major causes of unburned hydrocarbon formation.

The measured values of unburned hydrocarbon emission are presented in figure 5.

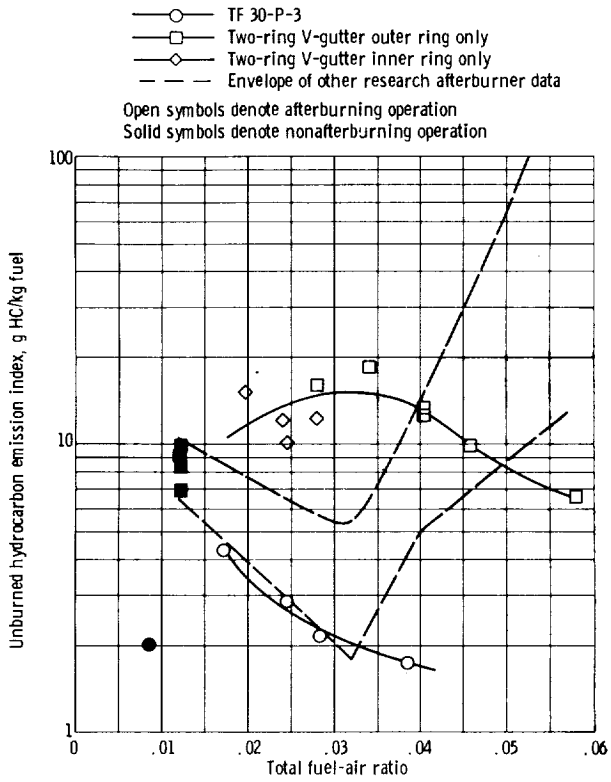


Figure 5. - Unburned hydrocarbon emission index.

The anomalous behavior of the research afterburner two-ring V-gutter, when compared with the other research afterburner designs, is not well understood. As before, the difference in the constituent emission level between the full-scale and research afterburner appears to be due to the variation in efficiency between the primary combustor and the preheater. A substantial amount of unburned hydrocarbon was measured for several of the other research afterburner designs.

## Hydrogen Emission

The presence of unburned hydrogen in concentrations greater than equilibrium predicted values was expected because of the afterburner's inefficient operation. Slightly less than 4 grams of $H_2$ per kilogram of fuel burned will be formed for each percent of inefficient operation due entirely to unburned hydrogen.

The measured values of unreacted hydrogen are presented in figure 6. The data

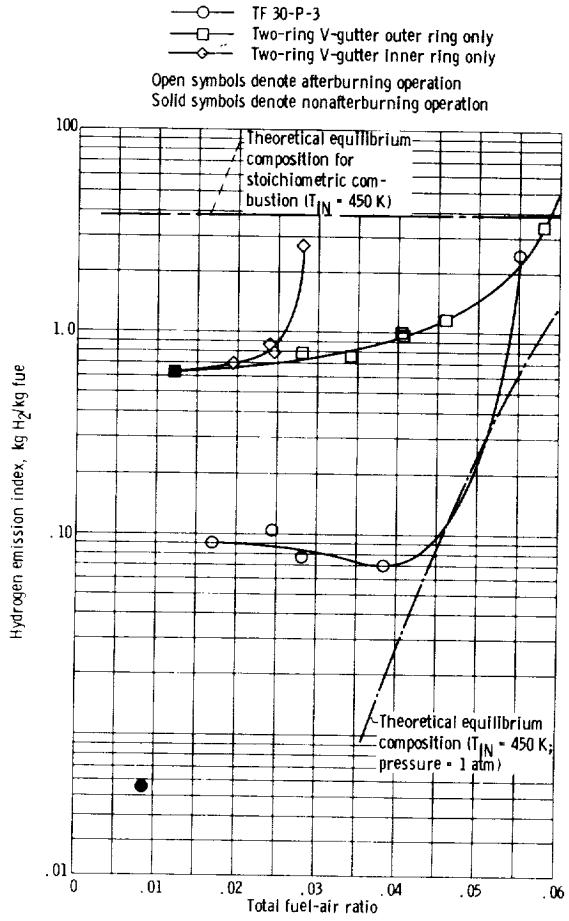


Figure 6. - Hydrogen emission index.

trends shown here closely follow the pattern of the CO emission; that is, as the afterburner fuel-air ratio is increased, the concentration of $H_2$ or CO increases markedly at some point. Again, the difference in overall level between the two configurations is primarily the difference in emissions produced by the primary combustor or preheater. As was the case with CO emission, research afterburner operation at low fuel-air ratios produced little change in the emission index (volumetric concentration increases as fuel-air ratio increases). The level of unburned products jumps significantly when the full-scale engine begins afterburning.

For the majority of the operating regime the inefficiency contribution due to unburned hydrogen is low, even though the quantity produced exceeds the theoretical equilibrium concentration.

## Sample Validity

Measured values of $CO_2$ emission are mainly used to check the sample validity. If the quantity of solid carbon particles is assumed to be negligible, then closure is obtained on the carbon atom system through the measured concentrations of CO, $CO_2$, and unburned hydrocarbon. One method of checking sample validity is to compute the local fuel-air ratio from the measured quantities. This value is then compared with the known fuel-air ratio. Another method involves predicting the measured $CO_2$ concentration by subtracting the CO concentration and the unburned hydrocarbon concentration from the theoretical equilibrium $CO_2$ values. The results of such a computation are shown in figure 7. In general, the agreement is poor, especially for the full-scale engine data.

Several inferences concerning the gas sampling techniques can be drawn from these data. Gas sampling may be improved with sample probes specifically designed for that purpose. The behavior of the research afterburner sample probe was consistent with its center-weighted design. For relatively homogeneous mixture, as in the nonafterburning data, agreement was good. Burning confined in the center of the duct produced very high measured concentrations; burning on the outer ring produced lower than ideal concentrations.

The full-scale engine afterburner presented additional difficulties because of its mixed flow character. In the nonafterburning case measured values are much higher than anticipated, indicating that the core flow was being preferentially weighted. Investigation of the afterburning data substantiate this hypothesis. Fuel zone 1 combustion occurs in the core-stream fan-stream boundary. As successively more fuel is introduced in the fan stream (zones 2 to 4), the deviation from ideal increases. When additional fuel is introduced into the core stream (zone 5) agreement is improved.

In light of this discussion, some additional comments on the data trends may be beneficial. The fact that the nonafterburning data for the TF30 turbofan was high as

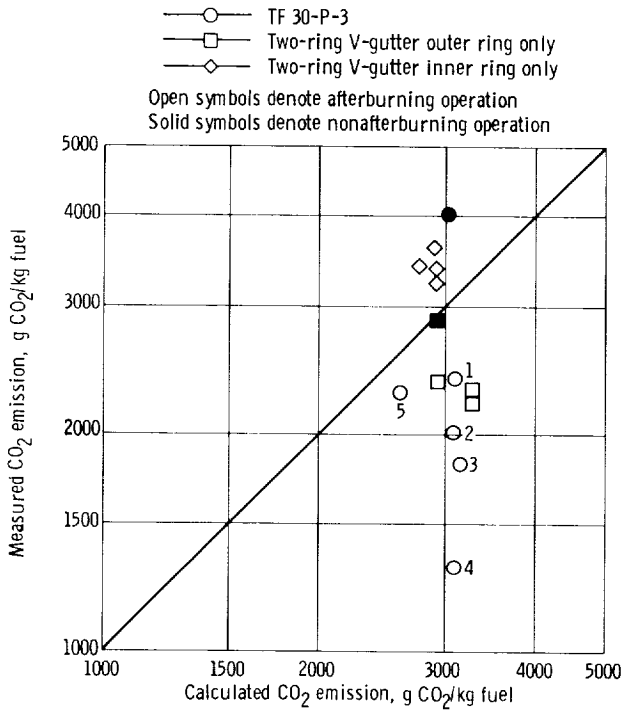


Figure 7. - Comparison of measured and calculated carbon dioxide emission. Numbers refer to TF 30-P-3 afterburner fuel zones.

shown in figure 7 may provide an additional reason for the higher NO emission level of the full-scale engine compared with that of the research afterburner. With afterburning, the unreacted constituents of CO, $H_2$, and hydrocarbons for the full-scale engine should be lower than that of the research afterburner on the basis of sampling error alone. This is verified in the data already presented.

## Comparison with Data from Reference 12

The data are compared in table III with turbofan and automobile engine data as presented in reference 12. The turbofan data are representative of engines such as the JT3D or JT8D; the automobile engine data are derived from the 1970 and 1971 emission standards. At idle conditions the TF30 compares favorably with other turbofan data, but at takeoff the TF30 samples showed higher values, perhaps, because of sampling errors as discussed previously.

TABLE III. - COMPARISON OF EXPERIMENTAL DATA WITH THAT OF REFERENCE 12

| Engine | Operating mode | Emission index, g/kg fuel | | |
|---|---|---|---|---|
| | | CO | Hydrocarbon | NO |
| Turbofan (ref. 12) | Idle | 50 - 174 | 10 - 75 | 2.0 |
| | Approach | 7 - 9 | 1 - 16 | 2.7 |
| | Takeoff | 0.7 - 1.2 | 0.1 - 0.6 | 4.3 |
| Automobile (ref. 12) | Overall average | 104 | 10 | 18 |
| TF30 nonafterburning | Idle[a] | 82 | 20 | 1.7 |
| | Takeoff[a] | 1.5 | 2.5 | 8.2 |
| | Altitude[b] | 4.2 | 2.0 | 7.8 |
| TF30-P-3 afterburner | Altitude[b] | 20 - 250 | 1.8 - 4.1 | 1 - 3.4 |
| J-57 research preheater | | 100 - 130 | 6 - 11 | 0.25 - 1.1 |
| Research afterburner | | 45 - 1600 | 2 - 100 | 0.1 - 1.5 |

[a]Data for idle and takeoff were taken during the test program but are not shown in the figures.

[b]Altitude data taken at a simulated engine inlet condition of Mach 1.3 flight at 12 200 m (40 000 ft).

## CONCLUDING REMARKS

Preliminary measurements of gaseous emissions from jet engine afterburners justify the supposition that they may be heavy pollution sources. The use of predicted emission concentrations based on theoretical equilibrium concentrations may be seriously in error. Measured values of emission index for carbon monoxide are substantially higher than for a nonafterburning engine. Unburned hydrocarbon emissions are also increased. Afterburner operation had little effect on nitric oxide emissions.

Caution is necessary when making comparisons between afterburning and nonafterburning engines on an emission index basis. Of primary interest is the total weight of each pollutant produced by an aircraft of given size. To obtain such a comparison between afterburning and nonafterburning engines, measurements should be taken at the same value of engine thrust. Because afterburning engines produce less thrust per pound of fuel burned, a given aircraft will consume more fuel with afterburning engines and will produce more pollution, relative to nonafterburning engines, than is indicated from a simple comparison of emission index data.

As only a limited amount of data have been gathered, only trends may be inferred. Considerably more data will be needed to establish consistent emission levels for afterburners. In addition, measurement techniques for use in turbofan mixed-flow afterburners have not been completely resolved. Improvements in gas sample probes and sample analysis are required. Furthermore, particulate measurements may also be a significant consideration.

Lewis Research Center,
National Aeronautics and Space Administration,
Cleveland, Ohio, April 16, 1971,
720-03.

## REFERENCES

1. Starkman, E.S.; Mizutani, Y.; Sawyer, R. F.; and Teixeira, D. P.: The Role of Chemistry in Gas Turbine Emissions. Paper 70-GT-81, ASME, May 1970.

2. Anon.: Nature and Control of Aircraft Engine Exhaust Emissions. Rep. 1134-1, Northern Res. and Eng. Corp., Nov. 1968.

3. Heywood, John B.; Fay, James A.; and Linden, Lawrence H.: Jet Aircraft Air Pollutant Production and Dispersion. Paper 70-115, AIAA, Jan. 1970.

4. Bristol, C. W., Jr.: Gas Turbine Engine Emission Characteristics and Future Outlook. Proceedings of a Combined Society of Automotive Engineers and U.S. Department of Transportation Conference on Aircraft and the Environment. SAE, 1971, pp. 84-92.

5. Swihart, John M.: The United States SST and Air Quality. Proceedings of a Combined Society of Automotive Engineers and U.S. Department of Transportation Conference on Aircraft and the Environment. SAE, 1971, pp. 93-102.

6. Anon.: Man's Impact on the Global Environment. MIT Press, 1970.

7. McAulay, John E.: Effect of Dynamic Variations in Engine-Inlet Pressure on the Compressor System of a Twin-Spool Turbofan Engine. NASA TM X-2081, 1970.

8. Saltzman, Bernard E.: Colorimetric Microdetermination of Nitrogen Dioxide in the Atmosphere. Anal. Chem., vol. 26, no. 12, Dec. 1954, pp. 1949-1955.

9. Zeleznik, Frank J.; and Gordon, Sanford: A General IBM 704 or 7090 Computer Program for Computation of Chemical Equilibrium Compositions, Rocket Performance, and Chapman-Jouguet Detonations. NASA TN D-1454, 1962.

10. Fletcher, Donald S.; and Heywood, John B.: A Model for Nitric Oxide Emissions from Aircraft Gas Turbine Engines. Paper 71-123, AIAA, Jan. 1971.

11. Brokaw, Richard S.; and Bittker, David A.: Carbon Monoxide Oxidation Rates Computed for Automobile Exhaust Manifold Reactor Conditions. NASA TN D-7024, 1970.

12. Grobman, Jack; Jones, Robert E.; Marek, Cecil J.; and Niedzwiecki, Richard W.: Combustion. Aircraft Propulsion. NASA SP-259, 1971, pp. 97-134.

NASA-Langley, 1971 —— 33 E-6256